International Journal of Non-Linear Mechanics 43 (2008) 1064 – 1073

Contents lists available at ScienceDirect

International Journal of Non-Linear Mechanics

journal homepage: www.elsevier.com/locate/nlm

# Elastic coiled-coils act as energy buffers in the ATP synthase

Sébastien Neukirch[a], Alain Goriely[b,*], Andrew C. Hausrath[c]

[a]Laboratoire de Modélisation en Mécanique, CNRS and Université Pierre et Marie Curie, Paris, France
[b]Program in Applied Mathematics, Department of Mathematics, BIO5 Institute, Tucson, AZ 85721, USA
[c]Department of Biochemistry and Molecular Biophysics, University of Arizona, Tucson, AZ 85721, USA

ARTICLE INFO

*Article history:*
Received 28 September 2007
Received in revised form 10 June 2008
Accepted 11 June 2008

*Keywords:*
Proteins
Coiled-coils
Rod
Kirchhoff equations
Energy transfer

ABSTRACT

In the ATP synthase, transmission of energy from the membrane-embedded F0 sector to the catalytic F1 sector is accomplished by two stalks composed of coiled-coils. The great efficiency of the enzyme, despite the presence of a symmetry mismatch between the F1 and F0 sectors, suggests the involvement of elastic elements that store energy during the catalytic cycle. Here, the stalk subunits $\gamma$ and $b$ are investigated as the source of this elastic compliance using a continuum mechanical model of coiled-coils and energy arguments. The analysis shows that the compliance of both subunits is required for efficient energy transmission between F0 and F1. In addition, the predicted mechanical properties of coiled-coils in the ATP synthase suggest mechanisms whereby regulatory subunits influence the enzyme activity.



The F1F0 ATP synthase is a multi-subunit enzyme complex that transduces energy stored as a transmembrane proton gradient into chemical energy in the form of adenosine triphosphate (ATP). A wealth of structural, biochemical and biophysical data are available for this remarkable enzyme [1–3]. The general structure of the bacterial enzyme is illustrated in Fig. 1. The membrane-embedded F0 sector is comprised of subunits *a*, *b*, and *c*, and the catalytic F1 sector is comprised of subunits $\alpha$, $\beta$, $\gamma$, $\delta$, and $\varepsilon$. Energy for ATP synthesis is obtained by translocating protons through a channel located at the interface of the *a* and *c* subunits in the F0 sector. Proton passage induces a rotation of the *c*-ring by one subunit thereby transducing the transmembrane proton gradient energy into rotary work. The $\gamma$ subunit then transmits this rotary work to the F1 sector. As the $\gamma$ subunit rotates, it interacts with the three catalytic $\beta$ subunits, yielding the release of newly synthesized ATP molecules. That is, the rotary work is converted into chemical potential energy [4]. The crystallographic structure of the $\gamma$ subunit shows that this mechanical linkage between F0 and F1 is accomplished through a left-handed coiled-coil [5].

The classic mechanical view of the enzyme presents the *c*-ring, the $\gamma$-shaft, and the $\varepsilon$ subunit as parts of a rotor subcomplex which rotates relative to the $ab_2\alpha_3\beta_3\delta$ subcomplex. The *a*, *b*, and $\delta$ subunits act as a stator which enables the rotor to exert torque on the catalytic $\beta$ subunits. No high-resolution structure is available for the complete F1F0 complex so the detailed molecular arrangement in the stator is not known. However, biochemical evidence shows that the two *b* subunits form a coiled-coil [7,8]. Therefore both linkages between the two energy-transducing components of this molecular machine appear to be composed of coiled-coils, which as described below, have mechanical properties exceptionally well-suited to this role.

The stoichiometry of proton usage in ATP synthesis has been a long-standing question [9]. For a mechanism where proton transport is strictly coupled to ATP synthesis, this question could be answered by determining the relative numbers of $\beta$ and *c* subunits within an active complex, as a single proton is passed by each *c* subunit and one ATP is produced by each $\beta$ subunit. The F1 sector contains three $\beta$ subunits and thus three active sites, but paradoxically the number of *c* subunits varies between organisms [10–13]. Crosslinking studies indicate that the *Escherichia coli* *c*-ring contains 10 subunits [10], and since a proton passage causes the *c*-ring to rotate by one unit, this single translocation event is associated with a rotation of $2\pi/10$ rad. This is the figure used for the rest of this paper. In a bacterium with a typical transmembrane proton-motive potential of 150 mV [14], each proton passage could supply as much as 150 meV. Under typical cellular ATP and ADP concentrations, ATP synthesis requires 12 kcal/mol, equivalent to $\sim$ 19 kT or $\sim$ 520 meV. Under these conditions, three proton translocations would not be sufficient to supply the necessary energy while four protons would supply 80 meV extra energy. Irrespective of the nature of catalytic events themselves, the

* Corresponding author.
*Abbreviations:* ATP, adenosine triphosphate ADP, adenosine diphosphate TF1, thermophilic F1 ATPase EF1*E. coli* F1 ATPase
*E-mail addresses:* sebastien.neukirch@lmm.jussieu.fr (S. Neukirch), goriely@math.arizona.edu (A. Goriely), hausrath@email.arizona.edu (A.C. Hausrath).

0020-7462/$ - see front matter © 2008 Elsevier Ltd. All rights reserved.
doi:10.1016/j.ijnonlinmec.2008.06.008

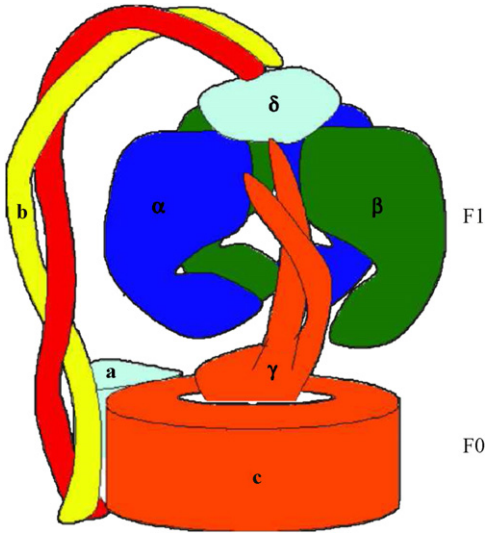


**Fig. 1.** *Cutaway schematic view of the F1F0 ATP synthase*. The *b* subunit comprising the stator is present in two copies in the complex and they are depicted here as a right-handed coiled-coil (red and yellow). (The structure of the *b* subunit in the intact complex is not known in detail, and the pitch and length of the $b_2$ coiled-coil portion have been exaggerated in this representation.) The $\gamma$ subunit (orange) forms a left-handed coiled-coil. The F0 sector transduces energy from proton translocation into rotational work which is used to drive catalysis in the F1 sector (from [6]).

enzyme must store and accumulate energy[1] from each individual proton passage until sufficient work has been done by the rotor to provide the necessary energy for ATP synthesis [18–24].

Central to this present work is the assumption that *the energy storage is achieved through the deformation of the coiled-coil stalk subunits $\gamma$ and b*. While it is clear based on kinetic arguments that such a storage element is needed for the observed efficiency [18], the actual location of this storage unit has not been definitely identified and remains controversial. Other possible locations include the $\beta$-sheet of the catalytic subunits [24] or the *c*-ring [12]. Here we follow Cherepanov et al. [18] in placing the elastic storage at the level of the stalks. Our objective is to examine the ability of an elastic coiled-coil model, applied to the *b* and $\gamma$ subunits, in fulfilling this elastic role. The mechanical response of these subunits to extension and twisting can be described quantitatively within a continuum elastic theory of protein coiled-coils [25]. We assume here that the elastic power transmission between the two motors of the ATP synthase is via the $\gamma$ and *b* coiled-coils. We are aware there are complications but, using this simple theory, we consider three scenarios for storing energy in F1F0:

H1. The *b* subunit is rigid, and energy is stored by coiling the $\gamma$ subunit alone.
H2. The *b* subunit is elastic and is anchored laterally on the $\alpha_3\beta_3$ subcomplex. Energy is stored by twisting $\gamma$ and stretching *b*.
H3. The *b* subunit is elastic and is anchored on the top of the $\alpha_3\beta_3$ subcomplex. Energy is stored by coiling both $\gamma$ and *b*: both subunits twist.

To test these hypotheses, we use the detailed mechanical, structural, and chemical information available and we analyze the energy balance of ATP synthase using a mechano-elastic description of the behavior of the $\gamma$ and $b_2$ coiled-coils.

[1] Unless the pore is leaky which is unlikely in view of the efficiency of the enzyme [15–17].

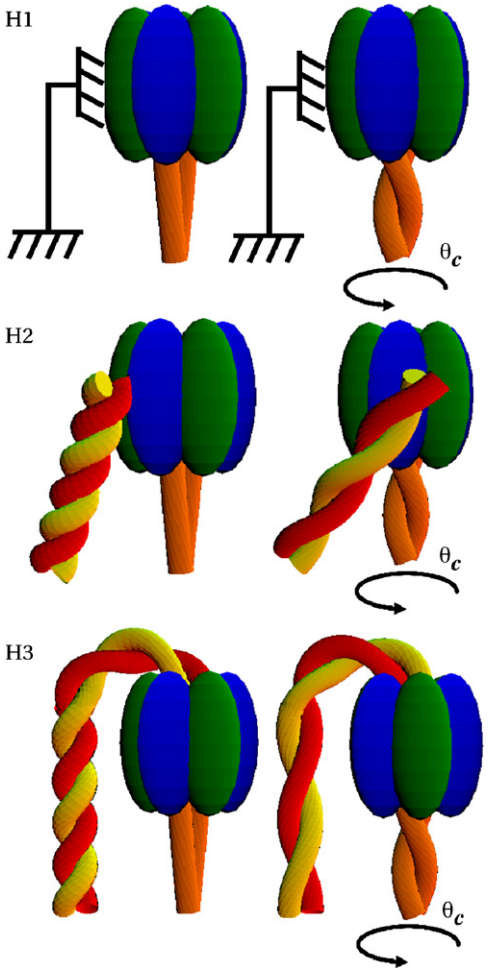


**Fig. 2.** *Three different possibilities for rotor–stator energy storage.* During proton translocation, in H1 (top) the rotor $\gamma$-shaft winds; in H2 (middle) the peripheral attachment for the *b* subunit primarily results in extensional deformation; in H3 (bottom) the axial attachment for the *b* subunit primarily results in torsional deformation. In H2 and H3, both rotor and stator act in concert.

## 1. Results

### 1.1. Testing H1: rigid b subunit and energy storage in the $\gamma$ subunit

The first hypothesis for the mechanism by which energy storage is accomplished is by overwinding of the $\gamma$ coiled-coil (see Fig. 2, top). Structural analyses have revealed that the $\gamma$ subunit coiled-coil can exist in different winding states [6,26,54] relative to that seen in the original structure [5]. The energy stored in the overwound $\gamma$ coiled-coil must approach 520 meV in order to have sufficient energy to synthesize one ATP. Applying an axial torque *M* on an elastic filament induces a rotation of the top with respect to the bottom. The rotational deformation in the filament is given by the *twist* $\tau$, that is the axial rotation per unit length. For low torque, the filament behaves linearly: the torque is equal to the twist times the *twist rigidity C*: $M = C\tau$. A typical value for the twist rigidity of an $\alpha$-helix is computed in [27] and evaluated to be $C_{\text{helix}} = 100\,\text{nm kT}$. We describe the mechanical response of a coiled-coil in terms of the mechanical properties of its constituent $\alpha$-helices: the twist rigidity *C* of the coiled-coil depends on the twist rigidities $C_{\text{helix}}$ of its components. In the regime where a coiled-coil is comprised of two $\alpha$-helices close to their natural state, the twist rigidity of the coiled-coil *C* is twice the twist rigidity of the constituent $\alpha$-helices: $C = 2C_{\text{helix}} = 200\,\text{nm kT}$.

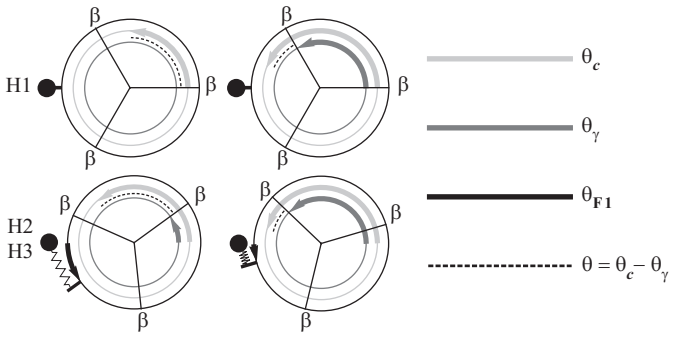


**Fig. 3.** *Definition of the angles for Hypotheses H1, H2, H3.* Top view looking down the axis of rotation of F1. From inside to outside the different rings correspond to the rotation of the top of the $\gamma$ subunit, the *c*-ring, and the $\alpha_3\beta_3$ hexamer. Under hypothesis H1, the hexamer is not allowed to rotate whereas in hypotheses H2 and H3, there is an elastic restoring force opposing the rotation of the hexamer. The dashed line corresponds to the rotation by an angle $\theta$ of the coiled-coil; that is, the twist present in the $\gamma$ coiled-coil. From left to right, the two diagrams show the configurations before and after of a synthetic event.

Then, the torque $M$ and the elastic strain energy $E_{\mathrm{el}}$ of a coiled-coil are

$$M = v\theta \quad \text{and} \quad E_{\mathrm{el}} = \tfrac{1}{2} v\theta^2, \tag{1}$$

where the linear coefficient of torque response $v$ for a coiled-coil of length $L$ is simply $v = C/L$. The total axial rotation imposed on the coiled-coil is $\theta = \tau L$, and $\theta = 0$ is the rest state. A coiled-coil can distribute deformation energy over its entire length. Eq. (1) implies that a longer coiled-coil is more compliant (smaller $v$) and so rotates more (larger $\theta$) under a given applied torque $M$. In our model of the ATP-synthase, the angle $\theta$ is the difference between the rotation $\theta_c$ of the *c*-ring and the rotation $\theta_\gamma$ of the top of the $\gamma$ coiled-coil as shown in Fig. 3.

We now estimate the elastic energy stored in the overwound conformation of $\gamma$ and compare it to the mechanical work produced by the enzyme. This energy can be estimated from experiments on the F1 motor, where the *b* subunit is not present and the observed torque is that exerted on $\gamma$ alone by the F1. The torque exerted during ATP hydrolysis by the isolated thermophilic F1 (TF1) reaches 40 pN nm under conditions where it appears that the enzyme is operating reversibly, at essentially 100 percent efficiency [28,29]. Therefore the reverse reaction, ATP synthesis in the intact F1F0, driven by mechanical rotation of the *c*-ring, should also operate under these conditions [17,30,31]. We assume that the torque delivered during these experiments is an intrinsic property of the F1 motor and that it functions with the same mechanics in vivo. This mechanistic view neglects possible experimental effects which might modify the torque values of the motor, such as attachment to a glass slide rather than to the stator.

The *E. coli* enzyme (EF1) appears to operate at a somewhat higher torque value of 63 pN nm [70]. In this organism, the *c*-ring consists of 10 units, so each proton passage induces a rotation of $2\pi/10$ rad which is transmitted to the $\gamma$-shaft. Energy is accumulated in the twisted shaft until enough is present to drive a catalytic event. At the other end of $\gamma$ there are three $\beta$ subunits in the F1 subcomplex, corresponding to a rotation of $2\pi/3$ rad for each ATP produced: when the $\gamma$-shaft is sufficiently twisted the active site is triggered: the shaft clicks round to the next active site, releasing enough energy to synthesize one ATP, and unwinding in the process.

The coiled-coil of $\gamma$ is left-handed and asymmetric. One strand spans residues 198–272 and the other approximately $\frac{2}{3}$ of that, residues 1–54. We use as an initial estimate for the length of the coiled-coil, the length of the shorter helix: 8 nm (assuming a rise of $h = 1.53$ Å per residue). Using Eq. (1) with $L = 8$ nm, and $C = 200$ nm kT, we evaluate the linear coefficient $v$ to be $v = 25$ kT. This implies a torque $M = 224$ pN nm, much larger than torques measured in single-molecule experiments [28,70], and a stored energy $E_{\mathrm{el}} = 55$ kT, nearly triple that needed for ATP synthesis.

However, deletions of segments at both the N- and C-terminus of the $\gamma$ subunit [43,44,69] are tolerated by the F1 enzyme and suggest that the upper portion of the stalk may be elastically irrelevant, and that the elasticity may arise from the *lower* portion, that part of $\gamma$ between the chemical and electrical motors, which has a length of $\sim$ 5 nm. Support for this conclusion is provided by the finding that some conserved contacts with the $\beta$ subunit in this region do not appear to influence torque generation [71]. The structure suggests that rotation of $\gamma$ is impeded by exerting torque on the lower domain of the $\beta$ subunit so that the upper part of $\gamma$ would be free-wheeling [47]. Finally, deletions in the lower portion of the coiled coil, to which we attribute the energy storage function, sharply curtail ATP hydrolysis in the chloroplast enzyme [46]. In this case, as the deformation would be distributed over a shorter elastic element ($L = 5$ nm), the compliance is decreased ($v = 40$ kT) and the predicted torque would be increased to $M = 359$ pN nm, and the stored energy would be 88 kT, well over four times that needed.

We conclude that the $\gamma$ subunit alone is too stiff to explain the observed properties of the enzyme. Therefore an additional elastic element, or energy storage mechanism, must come into play. We propose that the additional compliance is provided by the *b* subunit, so that the $2\pi/3$ rotation of the *c*-ring induces a lower twist of the $\gamma$-shaft, yielding a lower torque value.

### 1.2. The elastic b subunit participates in energy storing

While the identity of the stator subunits is clear, and partial structures of both the *b* and $\delta$ subunits are available [32–34], the detailed positions and conformations of these elements within the ATP synthase complex are still a subject of active investigation. In particular the mode of attachment of the stator to the $\alpha_3\beta_3$ subcomplex is unknown. Two distinct major models have been proposed. One proposes that the point of attachment is on the side of the $\alpha_3\beta_3$ subcomplex while the other proposes that the mechanical linkage is at the top [35–37]. Here we discuss the advantage of each model in explaining the mechanical properties of the enzyme and we present evidence that the energetics is more compatible with the latter model.

The *b* subunit of the *E. coli* enzyme is comprised of 156 residues. Subunit *b* is present in the F1F0 complex with a stoichiometry of 2 and when free in solution the membrane-extrinsic portion forms an elongated, $\alpha$-helical dimer, strongly suggesting a parallel, right-handed dimeric coiled-coil arrangement [7,38]. The $b_2$ coiled-coil spans the membrane, reaching from the bottom of the *c*-ring to the top of F1 [1,35]. An analysis of the mechanical coupling between $b_2$ and the $\alpha_3\beta_3$ subcomplex is not straightforward. When $\alpha_3\beta_3$ attempts to rotate due to torque produced in the F0 sector, an attachment point at the side of $\alpha_3\beta_3$ would subject the $b_2$ coiled-coil primarily to mechanical elongation (axial force) due to the lever-arm effect of $\alpha_3\beta_3$, as well as some twisting. Conversely, an attachment point near the top would subject $b_2$ primarily to twisting, with a small stretching component. Contrasting these two extremes, we make the simplifying assumptions that an attachment point at the side of $\alpha_3\beta_3$ would simply stretch the $b_2$ coiled-coil (Hypothesis H2) while an attachment point at the top would simply twist the $b_2$ coiled-coil (Hypothesis H3). We analyze the energetics of each mechanism in terms of the experimentally measured mechanochemistry of the ATP synthase.

The X-ray crystallographic structure of a construct consisting of *b* subunit residues 62–122 and subsequent biochemical studies led del Rizzo et al. to propose a parallel dimeric right-handed coiled-coil structure for the *b* subunit [8,33]. Here we use this model to

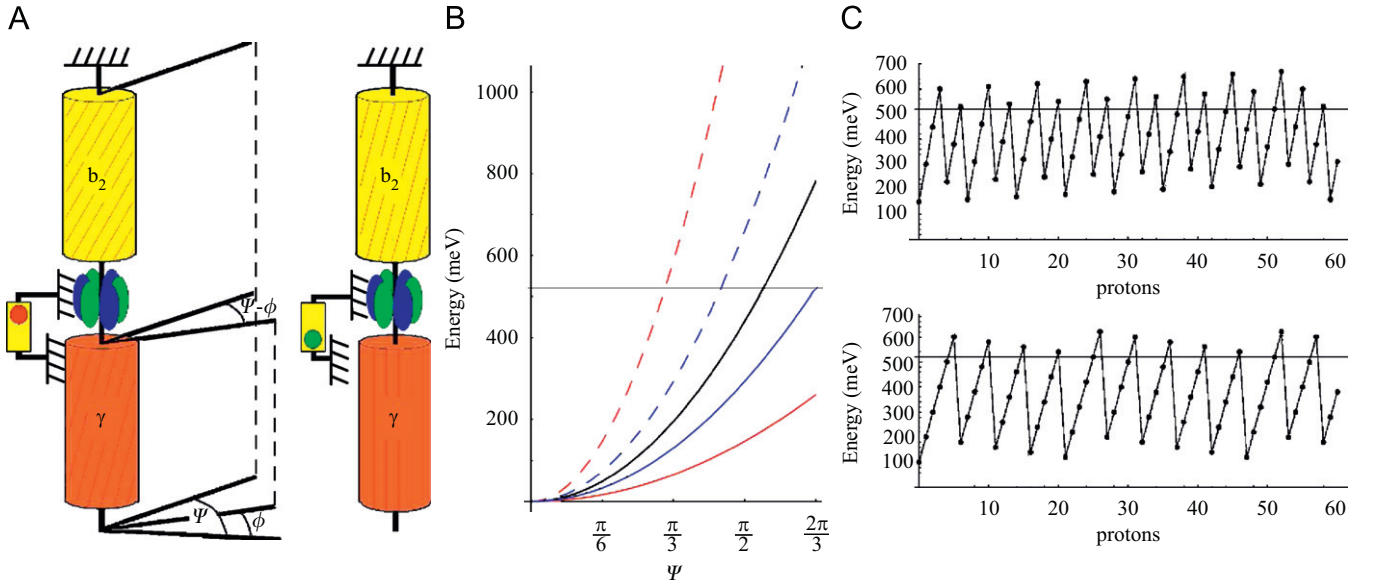


**Fig. 4.** *Continuum model of power transmission* (A): Mechanical schematic diagram with the elastic element representing $\gamma$ in orange and $b_2$ in yellow. The $\alpha_3\beta_3$ is between the two. The total twist in the combined element is $\psi$. The twist in $\gamma$ is $\phi$ and the twist in $b_2$ is $\psi-\phi$. (B): Work done on the combined element (black) as a function of the twist angle $\psi$. The energy stored in $\gamma$ and $b$ are in red and blue, respectively. The response of $\gamma$ alone (red dashed line), $b_2$ alone (blue dashed line), to the equivalent twist shows that the combined element is more compliant than either component in isolation. The effect of a decreased elastic constant is to broaden the energy well. (C): Energy stored in the combined elastic element vs protons utilized. Energy stored in the combined element increases until sufficient work is done (blue horizontal line) to allow the synthesis of ATP. Top and bottom display the response where proton passage delivers 150 or 100 meV, respectively.

analyze the mechanical properties of the structure. The portion of the molecule sufficient to mediate dimerization, residues 53–122 [7,39] is also assumed to be the coiled-coil segment dominating the mechanical properties of the stator. These 70 residues span approximately $L=10$ nm (assuming a rise of $h=1.53$ Å per residue). The structure of a coiled-coil has a non-linear influence on its elastic properties [25]. The presence of an undecad repeat in the sequence of the $b$ subunit, and detailed biochemical studies [7,8] indicate $b_2$ is a right-handed coiled-coil. This does not affect the twist stiffness of the shaft: $C_\gamma \simeq C_{b_2}$. Nevertheless, since $b_2$ is longer than $\gamma$, $b_2$ is more compliant than $\gamma$. That is, imposing a given rotation $\theta$ on $b_2$ is easier (i.e. achieved with lower torque $M$) than imposing the same rotation $\theta$ on $\gamma$, see Eq. (1). A coiled-coil responds to a stretching force by increasing its pitch. Consequently, $b_2$ being less steeply wound than $\gamma$ (i.e. having larger pitch), its propensity to extend is less than $\gamma$'s. In conclusion $b_2$ is easier to rotate than $\gamma$, but harder to extend. As the mechanical responses of the two coiled-coils is different, their combined influence could lead to asymmetric responses in F1F0.

### 1.3. Testing H2: energy storage shared by the $\gamma$ and $b$ subunits, $\gamma$ winds and $b$ stretches

In the case of a lateral attachment of the stator on the side of the $\alpha_3\beta_3$ subcomplex, the $b_2$ coiled-coil responds to rotation mostly by stretching. The $\alpha_3\beta_3$ subcomplex is schematically viewed as a sphere with radius $R=5$ nm and the $b_2$ coiled-coil is supposed as attached on its equator (see Fig. 2, middle). Depending on the length of the $b$ subunit and on the height of the attachment point, the $b$ subunit will stretch in different ways. Under application of a tensile force $F$, a coiled-coil stretches from its rest length $L$ to a length $L'$. We use a linear relation between the tensile force $F$ and the fractional extension $\varepsilon=(L'-L)/L$:

$$F=\mu\varepsilon \quad \text{and} \quad E=\tfrac{1}{2}\mu L\varepsilon^2, \tag{2}$$

where $\mu$ is the stretching modulus, the linear coefficient of force response, which is taken to be $\mu=1$ nN (see molecular mechanics simulations in [40]). The tensile force $F$ induces a torque (along the vertical) $M_b=RF$ on the $\alpha_3\beta_3$ subcomplex. This torque equilibrates with the torque of the $\gamma$-shaft. When the $c$-ring rotates (due to proton flux) through an angle $\theta$, this rotation is shared by the $\gamma$-shaft (which rotates by an angle $\theta_1$) and the $\alpha_3\beta_3$ subcomplex (which rotates by an angle $\theta_2$), with $\theta=\theta_1+\theta_2$. The respective values of $\theta_1$ and $\theta_2$ are selected by the equilibrium relation $M_\gamma=M_b$ where $M_\gamma=\nu\theta_1$ and $M_b=RF=R\mu\varepsilon$. The fractional extension $\varepsilon$ is a function of $\theta_2$: $\varepsilon=\varepsilon(\theta_2)$. This function is not easy to evaluate and we give two boundary scenarios in Appendix A. Nevertheless the angles $\theta_1$ and $\theta_2$ are solutions of the two equations $\theta=\theta_1+\theta_2$ and $\nu\theta_1=R\mu\varepsilon(\theta_2)$ which reduce to

$$\theta=\frac{R\mu}{\nu}\varepsilon(\theta_2)+\theta_2. \tag{3}$$

We want to solve (3) for $\theta_2$ when $\theta=2\pi/3$. The magnitude of the factor $R\mu/\nu\simeq 30$ (with $\nu=40$ kT) implies that $\theta_2$ is small (see Appendix A for examples). This means that the rotation $\theta$ is mainly distributed to $\theta_1$ which implies a torque $M_\gamma=\nu\theta_1$ on the $\gamma$ subunit (exerted by $b_2$) of approximately the same magnitude as in Hypothesis H1. Such a torque is too large compared to experimental measurements in $\gamma$ [28,29,70], as we saw in Section 1.1. We conclude that, due to the high stretching rigidity of the $b$ subunit, the enzyme in this proposed arrangement is not compliant enough to match the observed mechanical properties.

### 1.4. H3: energy storage shared by the $\gamma$ and $b$ subunits: both the $\gamma$ and $b$ subunits twist

We now consider the hypothesis that the rotational work done by the $c$-ring is distributed between the $\gamma$ and the $b$ subunits, with overwinding the $\gamma$ subunit but underwinding the $b_2$ coiled-coil (see Fig. 2 bottom). In the linear elastic regime, the effects of the two coiled-coils are additive and we can consider $b_2$ and $\gamma$ as a single coiled-coil of length $L=15$ nm, yielding a linear coefficient $\nu=13.3$ kT. The torque needed to achieve a $2\pi/3$ rotation on such a coiled-coil is $M=120$ pN nm and the stored energy is $E=29$ kT. This torque estimate is near the maximal measured torque (133 pN nm) in EF1 [70] and the

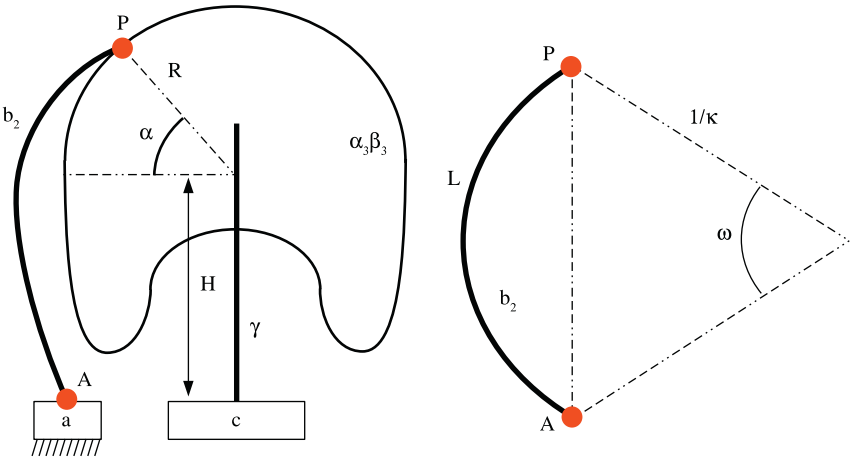


**Fig. 5.** *Transverse bending of the stator.* Left: the location of the attachment point $P$ of the $b$ subunit on the $\alpha_3\beta_3$ subcomplex varies with the height $H$ of the equator of the subcomplex and the latitude $\alpha$ of $P$. Right: when no rotation is present, the $b$ subunit, which has length $L > d(AP)$, is bent. This predicts the presence of an energy barrier for the reversal of the enzyme (see text).

energy is more than sufficient for ATP synthesis, suggesting that both coiled-coils are involved in the mechanical function of the enzyme and that an axial attachment model is favored energetically as it avoids the large energetic penalty for extension of the stator. The axial attachment also appears to be consistent with recent electron microscopy data (see Fig. 1 of [1]). (These estimates are somewhat higher than the values observed for TF1, but are still closer than that predicted for the arrangements described in Sections 1.1 and 1.3.)

The final model for the coupling in the ATP synthase is a pair of elastic filaments with torsional elastic constants $\nu_\gamma$ and $\nu_b$ connected in series (Fig. 4), with the $\alpha_3\beta_3$ complex in between them. Under proton passage, the $c$-ring and the $\gamma$-shaft rotate. The $\alpha_3\beta_3$ complex, which grips $\gamma$, is taken along and the rotation is eventually transmitted to $b_2$. Therefore the work done by proton passage is distributed between $\gamma$ and $b_2$. We define the angle $\psi$ as the overall twist in the combined element. It is the rotation of the $c$-ring relative to the $a$ subunit (the assumed anchor point of the $b_2$ element). The angle $\phi$ is the overall twist in $\gamma$, the rotation of the attachment point of $\gamma$ on $\alpha_3\beta_3$ relative to the $c$-ring. The overall twist in $b_2$ is the difference $\psi - \phi$. The total energy in the combined elastic system is obtained as the sum of the energies in the individual elements. Using Eq. (1), we have

$$E_{\text{tot}} = E_\gamma + E_b = \tfrac{1}{2}\nu_\gamma\phi^2 + \tfrac{1}{2}\nu_b(\psi-\phi)^2. \tag{4}$$

For fixed $\psi$, equilibrium requires the energy to be at a minimum:

$$\frac{\mathrm{d}E_{\text{tot}}}{\mathrm{d}\phi} = 0 \quad \text{so that } \phi = \frac{\nu_b}{\nu_b+\nu_\gamma}\psi.$$

and then

$$\psi - \phi = \frac{\nu_\gamma}{\nu_b+\nu_\gamma}\psi. \tag{5}$$

The partitioning of stored work between the two elastic elements is thus determined. The effective elastic constant of the two combined elements is

$$\nu_{\text{tot}} = \frac{\nu_b\nu_\gamma}{\nu_b+\nu_\gamma} \quad \text{so that } E_{\text{tot}} = \frac{1}{2}\nu_{\text{tot}}\psi^2. \tag{6}$$

The behavior of the effective elastic element and its components is displayed in Fig. 4B.

The model posits that the rotation of the $c$-ring stores energy in this combined element until sufficient energy is available for the synthesis of ATP. This work is distributed between the $\gamma$ and $b$ coiled-coils according to their individual compliances. When the stored energy is sufficient, the $\alpha_3\beta_3$ complex extracts the necessary amount from this energy buffer, decreasing the stored energy and allowing the top of $\gamma$ to rotate by $2\pi/3$ to the next active site, and concomitantly releasing ATP. The bottom of $\gamma$ is attached to the $c$-ring and does not rotate at the same time. Since the amount of energy in the buffer has changed, it then redistributes between the $b$ and $\gamma$ subunits. Further rotation of the $c$-ring therefore begins building up the stored energy from the residual left over from the previous catalytic event. The stored energy need not return to the same starting value each time. Therefore some catalytic events may require more additional energy input than others. Because the rotation of the $c$-ring takes place in discrete steps, this means that the stoichiometry of proton requirements per individual ATP is variable, although over many catalytic events the average must respect the conservation of energy.

### 1.5. The attachment point of the b subunit

Our model differs from that of del Rizzo et al. [8] in that we attribute the torsional strain to underwinding of the $b_2$ coiled-coil whereas in their model, torsional strain is assumed to be due to overwinding. In the linear regime, the magnitude of the deformation energy will be the same for over or underwinding, and so cannot be distinguished on these grounds. An attachment point close to the *north pole* ($\alpha = \pi/2$ in Fig. 5) results in underwinding. The conclusion from [8] that there is some overwinding of the $b_2$ coiled-coil is consistent with an attachment point close to the *equator* ($\alpha = 0$ in Fig. 5). Indeed, there is a latitude value, $0 < \alpha_0 < \pi/2$, at which rotation of the $\alpha_3\beta_3$ subcomplex will induce zero winding in the $b_2$ coiled-coil and thus the two models can be seen as limiting cases of a more general mechanism in which the attachment point would be at an intermediate latitude between the equator (Hypothesis H2) and the pole (Hypothesis H3). We have argued that the known energetics are consistent with the latter arrangement. But consideration of the mechanics in this hybrid model suggest some additional properties which are accessible to experiment. The geometry of the lateral attachment of the $b$ subunit induces a stretching force that has two components: a horizontal that builds up the torque on the $\alpha_3\beta_3$ subcomplex and a vertical component that tends to tilt the $\alpha_3\beta_3$ subcomplex. This tilt would tend to bend the $\gamma$-shaft.

For an attachment point $P$ of the $b$ subunit near the equator of the $\alpha_3\beta_3$ subcomplex, the $b$ subunit is bent when no rotation is present (see Fig. 5). The energy associated with this bending would oppose

reversal of the enzyme: this arrangement implies an "energy activation barrier" for switching between ATP synthesis and proton pumping modes, as explained in Section 2.4. To estimate the magnitude of this barrier, note that the length d($AP$) depends on the height $H$ of the equator of the $\alpha_3\beta_3$ subcomplex and on the latitude $\alpha$ of the attachment point $P$. Simple geometry yields $\mathrm{d}(AP)^2 = (H + R\sin\alpha)^2 + R^2(1-\cos\alpha)^2$, see Fig. 5, left. The shape of a slightly bent elastic filament compressed at both ends can be approximated by the arc of a circle. The bending energy is $E_b = (1/2)BL\kappa^2$ where $\kappa$ is the curvature of the bent filament and $B$ is its bending rigidity. For the $b_2$ coiled-coil, the bending rigidity $B$ is taken as approximately equal to the twist rigidity $B = C = 200\,\mathrm{nm\,kT}$. The curvature $\kappa$ of an arc of circle of length $L$ and chord $AP$ is the solution of equations:

$$\sin\omega = \kappa\,\mathrm{d}(AP)/2 \quad \text{and} \quad \omega = \kappa L/2. \tag{7}$$

When the curvature is small ($\kappa L \ll 1$), we have $\kappa^2 L^2 = 24(1 - \mathrm{d}(AP)/L)$. As an example, in the case $R = 5\,\mathrm{nm}$, $L = 10\,\mathrm{nm}$, $H = 6\,\mathrm{nm}$, and $\alpha = 45^\circ$ the value of the bending energy is $E_b = 8.5\,\mathrm{kT}$. This energy barrier has to be overcome when the enzyme reverses. Note that the $\gamma$ coiled-coil could bend also, so as to partly relieve the bending of the $b$ coiled-coil during this transition between modes, but the energy barrier would still be present.

## 2. Discussion

### 2.1. Role of elasticity in the efficiency of the ATP synthase

In the model presented here, the $b$ subunit is considered as a compliant element rather than as a rigid stator of the molecular motor. The true stator part is the $a$ subunit which is anchored in the membrane. The complementarity between the two coiled-coils during the loading process can help account for the efficiency of the enzyme. Under conditions where proton passage results in energy beyond that needed for synthesis, or in the case of an non-integer ratio between the number of $c$ and $\beta$ subunits [22], the excess (of rotation or energy) can be stored as torsional strain in the coiled-coils. However deformation of the $\gamma$-shaft alone could cause an angular mismatch between the rotation of the $c$-ring and the positions of the catalytic sites. Our Hypothesis H3 suggests that the torsional compliance of the $b$ subunit coiled-coil enables it to store (the major) part of the excess energy, allowing the $\gamma$-shaft to relax and restore the optimal angular relationship for synthesis. The $b$ subunit acts as an energy and torque buffer, maintaining a net torque on the F1 subcomplex, so that subsequent proton passages do not have to restore the applied torque from scratch to the level needed for synthesis. The activity of the ATP synthase is tolerant to changes in length of the $b$ subunit [41,42], which, in our model, corresponds to changes in the elastic properties of the $b_2$ coiled-coil (Eqs. (1) and (2)).

Since the isolated F1 appears to be a constant-torque motor, it is necessary that other parts of the synthase be able to deliver the appropriate torque. Functioning as energy accumulators, $b_2$ coiled-coils of different lengths will eventually achieve the torque needed for the mechanochemistry to proceed but would do so after different angular rotations of the $c$-ring.

In our model, the $\gamma$ subunit functions as an accumulator as well. As the function of an accumulator is predicted to be robust to changes in length, making insertions or deletions in the $\gamma$ coiled-coil would be an experimental means to test the proposed model. However, $\gamma$ must make interactions with both the $c$-ring at one end and $\alpha_3\beta_3$ at the other, and so much of $\gamma$ may be under additional functional constraints. Therefore insertions in the $\gamma$ stalk just below the portion contacting the $\alpha$ and $\beta$ subunits would be the best candidate locations for such a test. In contrast with the parallel coiled-coil in the $b$-stalk, which because of its dimeric nature can be extended with a single insertion, $\gamma$ contains an antiparallel coiled-coil and so an extension would require equal insertions in both helices, which would also have to be cleverly devised to maintain as much of the coiled-coil interface as possible. To our knowledge, experiments which change the length of the coiled-coil of $\gamma$ in this way have not been performed. As described above, deletions at the C-terminus of $\gamma$ (in the portion which extends past the coiled-coil) are tolerated and have minimal effect on torque [43,44]. This is likely because the upper portion is not subject to torsional strain, and is consistent with the notion that the accumulator function of $\gamma$ is localized within the lower portion.

Other sources of inefficiency could be unproductive proton transport or loss of energy during catalysis. The permanent presence of a torsional strain applied on the rotor would have the effect of suppressing rotational diffusion of the $c$-ring which could cause proton leakage. An additional consideration is that the torque-utilizing step in the ATP synthesis reaction might itself have an activation barrier. For such a mechanism the presence of an energy storage mechanism is necessary since there would have to be more energy in the rotor/stator combination than eventually used in the synthesis reaction. The height of this activation barrier could vary with environmental conditions (e.g. pH) independently of the mechanical constraints acting on the mechanism. Therefore the presence of such an activation barrier is a further requirement for an energy storage mechanism.

### 2.2. Comparison with other models

Detailed kinetic models of the ATP synthase mechanism have been devised. They accomplish the remarkable feat of reconciling the large body of experimental details about affinities, rates, torques, transport properties, and energetics which have been determined for this very complex enzyme (e.g. [18–20,45,47–50]). Most of these treatments employ elastic elements to treat the symmetry mismatch between F1 and F0. For example, the models in [18,19] employ a postulated elastic spring identified with the $\gamma$ subunit and are able to reproduce measured rates of ATP synthesis and hydrolysis and proton transport over a wide pH range with impressive accuracy. The authors noted that the elasticity in their model could have contributions from other subunits including $b$ and $\beta$. Other more structurally detailed models have analyzed the particular structural transitions taking place in the rotary mechanism in terms of rigid body domain motions connected by elastic hinges [47,50]. Again, these models have great explanatory power and can reconcile many diverse experimental details. But the source of the elasticity in these works was not treated explicitly. Our analysis seeks to understand the source of the assumed elastic properties in mechanical terms specific to the known structures. We find that an elastic treatment of deformations of the two coiled-coils in the two stalks of the ATP synthase is able to account for many of the mechanical properties of the enzyme.

Similar questions motivated a study by Sun et al. [24], following the work of Wang and Oster on the F1 ATPase [47], where a critical role for elasticity was demonstrated. It was determined by Sun et al. that the molecular basis of the elastic properties of F1 could be well described in terms of deformation of the $\beta$-sheet in the $\beta$ subunit. Their model suggests that ATP binding to an open $\beta$ subunit provides the energy to close the $\beta$ subunit, concomitantly deforming the $\beta$-sheet and driving the $\gamma$ subunit to the next position. In turn, $\gamma$ opens the subsequent $\beta$ subunit and releases the bound ADP, assisted by the transition of the $\beta$-sheet from the deformed closed position to the relaxed open conformation. (This is consistent with the open conformations of the $\beta$ subunits in the structure of the nucleotide-free $\alpha_3\beta_3$ complex [51].) In the ATP synthesis reaction our coiled-coil theory complements the work of Sun et al. The energy to close the $\beta$ subunit is supplied by binding ADP and Pi. In the bound form these reactants equilibrate rapidly with ATP [52]. The pre-strained

$\beta$ subunit is already closed and so lacks a degree of freedom in which to store energy in excess of that required to achieve the closed conformation. So when torque is supplied to $\gamma$, strain accumulates *in the stalk* until a point is reached where the $\beta$ subunit opens, ATP is released, and $\gamma$ is able to progress to the next position. In this picture, the accumulation of strain during ATP *synthesis* is not in the $\beta$ subunit but rather in the stalk subunits.

### 2.3. Structural evidence for elastic behaviour

Elasticity is introduced in the present mechanical model of the enzyme through the linearly elastic response of two coiled-coils ($\gamma$ and $b_2$) present in the structure. The presence of two elastic shafts provides a decoupling between the rotation of the *c*-ring and the rotation of the $\alpha_3\beta_3$ subcomplex, decreasing the importance of the relative stoichiometry of the *c* and $\beta$ subunits. Evidence for the elastic behavior of the $\gamma$-shaft is provided by crystal structures showing different winding states for the $\gamma$ subunit, supporting the notion of torsional elasticity [6,26,53,54]. In addition, other F1 crystal structures in which $\gamma$ is partially disordered support the conclusion that the native state of this subunit has intrinsic flexibility [5,55,56]. A monomeric crystal structure of the soluble portion of the *b* subunit revealed a straight helix [33]. Detailed biophysical and biochemical investigations proved that the solution conformation is a coiled-coil, documenting the elastic nature of the *b* subunit and showing that it also can flex while remaining in the folded conformation [8,33].

The proposed elastic energy buffer mechanism depends on geometrical parameters which can vary smoothly rather than in discrete jumps, so as to accommodate the different mechanical constraints on the model. It was observed by electron microscopy [57,58] that the distance between F1 and F0, parameter $H$ in our model, could change by 1–2 nm under different solution conditions which may reflect different modes of operation. These observations provide strong evidence that the stalk subunits are flexible, but the structural nature of the deformations are not clear at this resolution. The observed changes in $H$ may be associated with the bending of $\gamma$ and/or $b_2$. In our model, a change in the location of the attachment point of the *b* subunit on the $\alpha_3\beta_3$ subcomplex (selected by the parameters $H$ and $\alpha$) induces different responses of the rotor. Additionally, a more detailed analysis of coiled-coil mechanical properties shows there is a coupling between twisting and extension [25,59]. The observed changes in distance between F1 and F0 may reflect contributions from this effect.

The model describes the mechanical behavior of the stalk subunits in terms of elastic filaments with an assumed elastic constant. In this description the elastic response is homogeneously distributed throughout the filament and does not take into account local variations. Rather, it uses an overall resultant flexibility which results from the combined influence of the many local interactions contributing to the stability of the structure. We have used an elastic constant value of $C_{\text{helix}} = 100\,\text{nm}\,\text{kT}$ which is an estimate for the flexibility of a generic $\alpha$-helix [27]. However there are additional interactions particular to both the $\gamma$ and *b* subunits which are not taken into account when using this value. For example, the elasticity of $\gamma$ may be due in part to the presence of proline 44 (using *E. coli* numbering) which introduces a kink in the N-terminal helix and could introduce additional flexibility to this helix of the coiled-coil. If so, the effect of this proline residue within the model would be to reduce the elastic constant. Also present in the $\gamma$ subunit are various hydrogen bonding and salt bridge interactions, some of which stabilize the more tightly wound conformations, and others which stabilize the loosely wound conformations. The effect of such interactions on the elastic constant depends on the relative stabilization of the over and underwound conformations. If the more tightly wound states form interactions not present in the loosely wound states, the conformations at higher twist would be stabilized. Such a coiled-coil would less effectively oppose twist, and would be described with a lower elastic constant. A lower elastic constant in $\gamma$ would decrease the need for the additional elastic element as described in Section 1.1. Although we have inferred the elastic properties indirectly in the present work, with modern single-molecule techniques, it might be possible to measure the elastic response of the $\gamma$ subunit directly using mutants in which rotation is prevented [72,73].

In the *b* subunit, interactions with the side of $\alpha_3\beta_3$ (independent of the point of mechanical attachment) could stabilize either the over and underwound states of $b_2$ and so could potentially either increase or decrease the elastic constant. Our objective here is not to provide a detailed molecular description but rather examine how the overall architecture of the stalk subunits may contribute to elastic properties. As attested by the tolerance to insertions in the *b* subunit, it may be functionally less important what the particular resistance to torque is, and more important what range of torque can be accommodated. On a more general level, a continuum mechanical description of the energetics is akin to a thermodynamic description, in that much can be learned knowing the magnitudes of the energies involved in the process, even in the absence of a complete understanding of their microscopic origin.

### 2.4. Regulation and reversal

The requirement for the presence of a stator indicates that the synthetic apparatus of F1F0 can only function against a particular range of torque. Additionally, the isolated F1-ATPase delivers a constant torque irrespective of the load [28]. Therefore the mechanochemistry in either direction requires a mechanism to ensure that the torque is in the proper range. Our model posits that strain builds up in the coiled-coils until this range of torque is reached. We now consider how this energy storage role offers insights into possible regulatory mechanisms.

Under conditions of greatly diminished proton-motive force, more protons are needed to accumulate sufficient energy for synthesis of ATP and so larger angular displacements of the *c*-ring will be required. The reciprocity between the stalks (i.e. the mechanism by which overwinding of $\gamma$ is opposed by underwinding of $b_2$) may result in a significant underwinding of the $b_2$ coiled-coil which could play a role in determining the mode of operation of the enzyme. Underwinding of $b_2$ which is anchored to the *a* subunit could change the disposition of the proton pore at the interface of the *a* and *c* subunits so as to drive rotation of the *c*-ring in the opposite sense (cf. [60, Fig. 14]). In turn this would maintain the reversed conformation of the *b* subunit until the proton-motive force is restored and the enzyme can revert to ATP synthesis. Therefore the mechanical properties of coiled-coils provide a possible mechanism for adaptation to diminished membrane potential during ATP synthesis, as well as a mechanism for maintaining the proton gradient under a variety of steady state conditions.

The mechanism of switching between ATP synthesis and hydrolysis may also be analyzed based on this mechanical picture. As explained in Section 1.5, if the attachment point of the *b* subunit is placed somewhere in between the equator and the pole (see Fig. 5) the rotation of the $\alpha_3\beta_3$ subcomplex will induce both coiling and stretching of the $b_2$ coiled-coil which would work as described in Scenario B of the Appendix. In the forward gear, when producing ATP, the *b* subunit would work as in Fig. 7, right. When working in the reverse direction the points $P$ and $P'$ would be on the other side of the $\alpha_3\beta_3$ subcomplex. It is then easy to see that to go from one position to the other, the *b* subunit has to pass through a conformation where it is bent (Fig. 7, left or Fig. 5). Ultimately the ATP synthase is an enzyme which equilibrates ATP levels with the proton gradient. Thus switching to proton pumping mode should be favored when

ATP concentrations are relatively high but the transmembrane voltage is low. When this occurs, binding of ATP to the $\alpha_3\beta_3$ subcomplex applies torque to $\gamma$ and induces it to rotate, but the energy and torque made available have to first overcome the bending energy barrier of the $b$ subunit, before subsequent ATP turnovers can be utilized for proton transport. The bending energy in the intermediate configuration acts as an energy barrier preventing the enzyme from reversing erratically. Indeed, depending on the value of $\alpha$ and $H$, this energy barrier can vary from zero to few $kT$. Note that in the eukaryotic ATP synthases, there are additional regulatory subunits associated with the stalk, which may act to modulate this energy barrier by binding and stabilizing either the straight or bent conformation of the stalk [61].

A similar mechanism may also occur in the central stalk. The regulatory $\varepsilon$ subunit has long been known as an inhibitor of ATPase activity [58,62,63], which was difficult to reconcile with its location at the base of the central stalk, over 50 Å distant from the catalytic centers in F1 [6,53]. Subsequent structural and biochemical work revealed a dramatic conformational rearrangement of its C-terminal helical hairpin domain [64–66] which reaches up from the base of the $\gamma$ coiled-coil to interact with the $\alpha_3\beta_3$ hexamer, possibly influencing the catalytic properties of the active sites. In this conformation $\varepsilon$ also serves to prevent backward rotation and ATP hydrolysis [67,68], but the mechanism by which this is accomplished is less clear. It is interesting to note that before these studies were available, based purely on kinetic grounds Cherepanov et al. delineated the mechanical prerequisite that there be asymmetry between the synthesis and hydrolysis directions, postulating that "the averaged elastic state during the turnover of ATP synthase is expected to differ from that of ATPase" [18]. We conclude with the proposition that under synthesis conditions the extended C-terminal helix of $\varepsilon$ incorporates into the $\gamma$ coiled coil, forming a three-stranded $\gamma/\varepsilon$ coiled-coil. ATP synthesis occurs at higher values of the proton-motive force. Therefore optimal mechanical functions require a stiffer coupling to transmit higher torque available from a single proton passage. Mechanically, a three-stranded coiled-coil is stiffer than a two-coiled-coil. Therefore, the switch between two and three strands would significantly stiffen the central stalk and introduce the necessary mechanical asymmetry.

## Acknowledgments

A.H. and A.G. acknowledge support for this work through a grant from the Bio5 Institute, and A.H. also thanks the Department of Biochemistry and Molecular Biophysics, University of Arizona. This material is based in part upon work supported by the National Science Foundation under Grant nos. DMS-0604704 and DMS-IGMS-0623989 to A.G.

## Appendix A. Two scenarios for the stretching of $b$

Depending on the length $L$ of the $b$ subunit and on the height $H$ of the equator of the $\alpha_3\beta_3$ subcomplex, the $b$ subunit will stretch in different ways. We study two scenarios where $b$ is attached on the equator of $\alpha_3\beta_3$, seen as a sphere of radius $R = 5$ nm. The two scenarios differ in the height $H$.

### A.1. Scenario A

Here the height of the equator of the $\alpha_3\beta_3$ subcomplex is equal to the length of the $b$ subunit ($H = L$). Consequently when $\alpha_3\beta_3$ is not rotated, $b$ is straight. A rotation, of an angle $\theta$ around the vertical, of the $c$-ring induces a torsion in the $\gamma$-shaft (of angle $\theta_1$) and a rotation (of angle $\theta_2$) of the $\alpha_3\beta_3$ subcomplex. Consequently the attachment point $P$ of the $b$ subunit moves, thereby stretching it from length $L$ to length $L'$. The two rotations $\theta_1$ and $\theta_2$ add up to $\theta$ the rotation of the $c$-ring : $\theta = \theta_1 + \theta_2$. The torque in the $\gamma$-shaft is $M_\gamma = \nu\,\theta_1$ and the torque exerted by the stretching force $F$ in the $b$ subunit is $M_b = RF\sin\theta_3$ (where $\theta_3$ is the tilt of the $b_2$ coiled-coil). To relate the extension $\varepsilon$ of the $b$ subunit to the rotation $\theta_2$ of the $\alpha_3\beta_3$ subcomplex, note that $R\theta_2 \simeq L\theta_3$ and $L' = L/\cos\theta_3$, see Fig. 6, right. This implies a fractional extension:

$$\varepsilon(\theta_2) \stackrel{\text{def}}{=} \frac{L'}{L} - 1 = \frac{1}{\cos\theta_3} - 1 \left(\simeq \frac{1}{2}\left(\frac{R}{L}\right)^2 \theta_2^2\right) \tag{8}$$

and the equilibrium equation $M_b = M_\gamma$ reads

$$\theta = \frac{R\mu}{\nu}\left\{\tan\left(\frac{R}{L}\,\theta_2\right) - \sin\left(\frac{R}{L}\,\theta_2\right)\right\} + \theta_2 \tag{9}$$

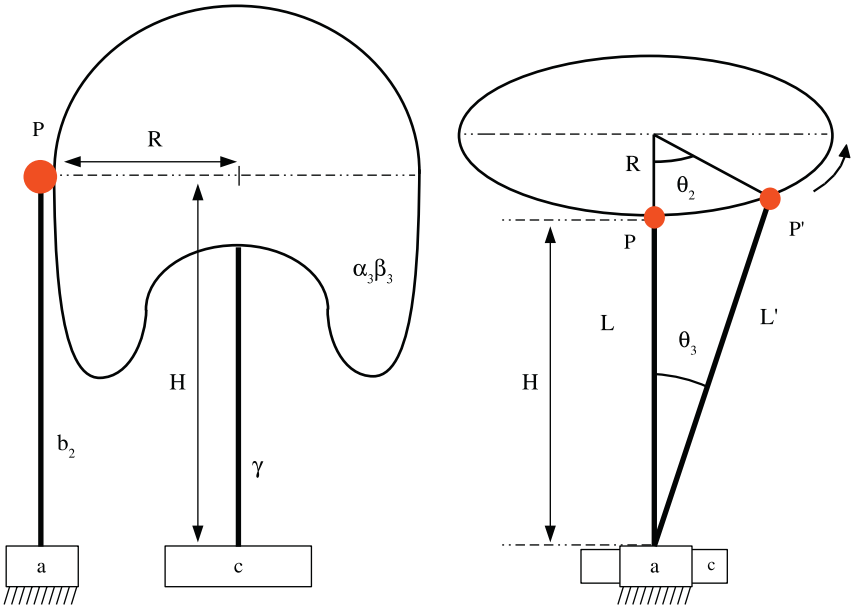


**Fig. 6.** *Stator attachment scenario A* conformation of the enzyme in the case where the length $L$ of the $b$ subunit is equal to the height of the attachment point $P$. Left: when no rotation is present. Right (side view): when the $c$-ring and $\alpha_3\beta_3$ subcomplex rotate, the $b$ subunit is stretched to a length $L'$.

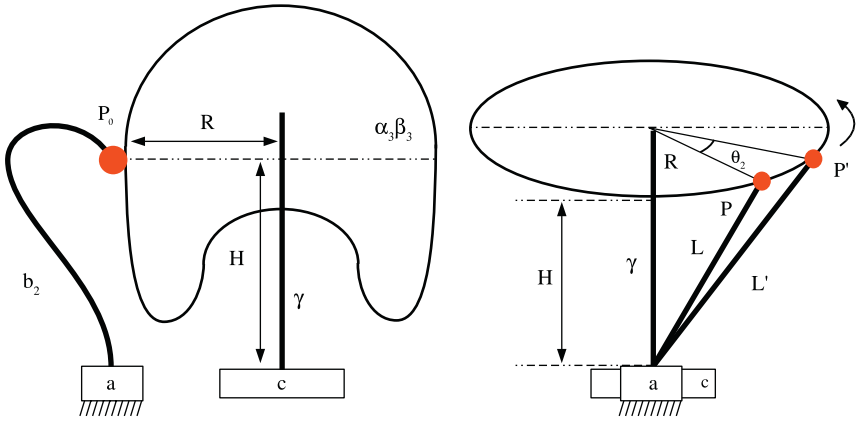


**Fig. 7.** *Stator attachment scenario B* conformation of the enzyme in the case where the length $L$ of the $b$ subunit is larger than the height $H$ of the equator of the $\alpha_3\beta_3$ subcomplex. Left: when no rotation is present the $b$ subunit is bent. Right (side view): when the $c$-ring and $\alpha_3\beta_3$ subcomplex rotates, the $b$ subunit is stretched to a length $L'$.

which is solved to yield $\theta_2 = 0.86$ rad with $\theta = 2\pi/3$, $R\mu/v = 30$ and $L = 10$ nm. This implies $\theta_1 = 1.24$ rad which yields a torque in the $\gamma$-shaft $M_\gamma = 206$ pN nm and stored energies of $E_b = \frac{1}{2}\mu L\varepsilon^2 = 11.5$ kT and $E_\gamma = \frac{1}{2}v\theta_1^2 = 30$ kT.

This means that when the $c$-ring rotates by an angle $\theta = 2\pi/3$, $\gamma$ rotates by an angle $\theta_1 = 1.24$ rad and the torque $M_\gamma$ created by this rotation is above the maximal measured value [70]. In conclusion we see that the compliance due to the $b$ subunit (by comparison with a totally rigid $b$ subunit, see Section 1.1) is not sufficient to lower the torque present in the $\gamma$ shaft so as to match the experimentally observed values.

### A.2. Scenario B

Here the $b$ subunit is attached in the same manner as in the previous case but the height $H$ of the equator is reduced in such a way that when $\alpha_3\beta_3$ is not rotated with regard to the $a$ subunit, the $b$ subunit is bent (see Fig. 7, left). A rotation of the $\alpha_3\beta_3$ subcomplex is needed to straighten the $b$ subunit. We define this point as the rest point and consider the effect of stretching $b$ from this point.

In this case a rotation $\theta_2$ of the $\alpha_3\beta_3$ subcomplex will induce a larger stretch of the $b$ subunit than in the previous scenario: for example if the height $H$ is small compared to $L$, a rotation $\theta_2$ implies $L' - L \simeq R\theta_2$ and $\varepsilon(\theta_2) \simeq (R/L)\theta_2$, larger than (8). The equilibrium equation reads

$$\theta \simeq \frac{R\mu}{v}\frac{R}{L}\theta_2 + \theta_2 \simeq 16\theta_2 \tag{10}$$

which yields $\theta_2 = 0.13$ rad. A refined (though not exact) geometrical picture (see Fig. 7, right) yields the following equation:

$$\theta = \frac{R\mu}{v}\left(\frac{1}{L} - \frac{1}{\sqrt{R^2\theta_2^2 + L^2 + 2R\theta_2\sqrt{L^2 - H^2}}}\right) \times (R\theta_2 + \sqrt{L^2 - H^2}) + \theta_2 \tag{11}$$

which solves to $\theta_2 = 0.19$ rad for $H = 6$ nm. In this case $\theta_1 = 1.91$ rad and $M_\gamma = 318$ pN nm which is too large compared to the maximal experimental value reported in [70]. The energies stored in the two elastic units are: $E_\gamma = \frac{1}{2}v\theta_1^2 = 71$ kT and $E_b = \frac{1}{2}\mu L\varepsilon^2 = 6.8$ kT. We conclude that this set up does not produce the appropriate compliance.

## References

[1] S. Wilkens, F1F0-ATP synthase—stalking mind and imagination, J. Bioenerg. Biomembranes 32 (4) (2000) 333–339.
[2] A.E. Senior, S. Nadanaciva, J. Weber, The molecular mechanism of ATP synthesis by F1F0-ATP synthase, Biochim. Biophys. Acta Bioenerg. 1553 (3) (2002) 188–211.
[3] P.D. Boyer, The ATP synthase—a splendid molecular machine, Annu. Rev. Biochem. 66 (1997) 717–749.
[4] D. Stock, C. Gibbons, I. Arechaga, A.G.W. Leslie, J.E. Walker, The rotary mechanism of ATP synthase, Curr. Opinion Struct. Biol. 10 (6) (2000) 672–679.
[5] J.P. Abrahams, A.G.W. Leslie, R. Lutter, J.E. Walker, Structure at 2.8-angstrom resolution of F1-ATPase from bovine heart-mitochondria, Nature 370 (6491) (1994) 621–628.
[6] D. Stock, A.G.W. Leslie, J.E. Walker, Molecular architecture of the rotary motor in ATP synthase, Science 286 (5445) (1999) 1700–1705.
[7] M. Revington, S.D. Dunn, G.S. Shaw, Folding and stability of the $b$ subunit of the F1F0 ATP synthase, Protein Sci. 11 (5) (2002) 1227–1238.
[8] P.A. del Rizzo, Y. Bi, S.D. Dunn, ATP synthase $b$ subunit dimerization domain: a right-handed coiled coil with offset helices, J. Mol. Biol. 364 (4) (2006) 735–746.
[9] J.J. Tomashek, W.S.A. Brusilow, Stoichiometry of energy coupling by proton-translocating ATPases: a history of variability, J. Bioenerg. Biomembranes 32 (5) (2000) 493–500.
[10] W.P. Jiang, J. Hermolin, R.H. Fillingame, The preferred stoichiometry of $c$ subunits in the rotary motor sector of *Escherichia coli* ATP synthase is 10, Proc. Natl. Acad. Sci. USA 98 (9) (2001) 4966–4971.
[11] J.S. Lolkema, E.J. Boekema, The A-type ATP synthase subunit K of *Methanopyrus kandleri* is deduced from its sequence to form a monomeric rotor comprising 13 hairpin domains, FEBS Lett. 543 (1–3) (2003) 47–50.
[12] T. Meier, P. Polzer, K. Diederichs, W. Welte, P. Dimroth, Structure of the rotor ring of F-type Na+-ATPase from *Ilyobacter tartaricus*, Science 308 (5722) (2005) 659–662.
[13] D. Pogoryelov, J.S. Yu, T. Meier, J. Vonck, P. Dimroth, D.J. Muller, The $c(15)$ ring of the *Spirulina platensis* F-ATP synthase: F-1/F-0 symmetry mismatch is not obligatory, Embo Rep. 6 (11) (2005) 1040–1044.
[14] E.R. Kashket, The proton motive force in bacteria: a critical assessment of methods, Annu. Rev. Microbiol. 39 (1985) 219–242.
[15] K. Kinosita, R. Yasuda, H. Noji, K. Adachi, A rotary molecular motor that can work at near 100 percent efficiency, Philos. Trans. R. Soc. London Ser. B Biol. Sci. 355 (1396) (2000) 473–489.
[16] G. Oster, H.Y. Wang, Why is the mechanical efficiency of F-1-ATPase so high?, J. Bioenerg. Biomembranes 32 (5) (2000) 459–469.
[17] Y. Rondelez, G. Tresset, T. Nakashima, Y. Kato-Yamada, H. Fujita, S. Takeuchi, H. Noji, Highly coupled ATP synthesis by F-1-ATPase single molecules, Nature 433 (7027) (2005) 773–777.
[18] D.A. Cherepanov, A.Y. Mulkidjanian, W. Junge, Transient accumulation of elastic energy in proton translocating ATP synthase, FEBS Lett. 449 (1) (1999) 1–6.
[19] O. Panke, B. Rumberg, Kinetic modeling of rotary CF0F1-ATP synthase: storage of elastic energy during energy transduction, Biochim. Biophys. Acta Bioenerg. 1412 (2) (1999) 118–128.
[20] W. Junge, O. Panke, D.A. Cherepanov, K. Gumbiowski, M. Muller, S. Engelbrecht, Inter-subunit rotation and elastic power transmission in F0F1-ATPase, FEBS Lett. 504 (3) (2001) 152–160.
[21] O. Panke, D.A. Cherepanov, K. Gumbiowski, S. Engelbrecht, W. Junge, Viscoelastic dynamics of actin filaments coupled to rotary F-ATPase: angular torque profile of the enzyme, Biophys. J. 81 (3) (2001) 1220–1233.
[22] N. Mitome, T. Suzuki, S. Hayashi, M. Yoshida, Thermophilic ATP synthase has a decamer $c$-ring: indication of noninteger 10:3 H+/ATP ratio and permissive elastic coupling, Proc. Natl. Acad. Sci. USA 101 (33) (2004) 12159–12164.
[23] M.S. Liu, B.D. Todd, R.J. Sadus, Kinetics and chemomechanical properties of the F-1-ATPase molecular motor, J. Chem. Phys. 118 (21) (2003) 9890–9898.
[24] S. Sun, D. Chandler, A.R. Dinner, G. Oster, Elastic energy storage in beta-sheets with application to F-1-ATPase, Eur. Biophys. J. Biophys. Lett. 32 (8) (2003) 676–683.

[25] S. Neukirch, A. Goriely, A.C. Hausrath, Chirality of coiled-coils: elasticity matters, Phys. Rev. Lett. 100 (2008) 038105.
[26] A.C. Hausrath, R.A. Capaldi, B.W. Matthews, The conformation of the epsilon-and gamma-subunits within the *Escherichia coli* F-1 ATPase, J. Biol. Chem. 276 (50) (2001) 47227–47232.
[27] S. Choe, S.X. Sun, The elasticity of alpha-helices, J. Chem. Phys. 122 (2005) 244912.
[28] R. Yasuda, H. Noji, K. Kinosita, M. Yoshida, F1-ATPase is a highly efficient molecular motor that rotates with discrete 120° steps, Cell 93 (1998) 1117–1124.
[29] H. Omote, N. Sambonmatsu, K. Saito, Y. Sambongi, A. Iwamoto-Kihara, T. Yanagida, Y. Wada, M. Futai, The gamma-subunit rotation and torque generation in F-1-ATPase from wild-type or uncoupled mutant *Escherichia coli*, Proc. Natl. Acad. Sci. USA 96 (14) (1999) 7780–7784.
[30] Y. Hirono-Hara, K. Ishuzuka, K. Kinosita, M. Yoshida, H. Noji, Activation of pausing F-1 motor by external force, Proc. Natl. Acad. Sci. USA 102 (12) (2005) 4288–4293.
[31] H. Itoh, A. Takahashi, K. Adachi, H. Noji, R. Yasuda, M. Yoshida, K. Kinosita, Mechanically driven ATP synthesis by F-1-ATPase, Nature 427 (6973) (2004) 465–468.
[32] O. Dmitriev, P.C. Jones, W.P. Jiang, R.H. Fillingame, Structure of the membrane domain of subunit *b* of the *Escherichia coli* F0F1 ATP synthase, J. Biol. Chem. 274 (22) (1999) 15598–15604.
[33] P.A. del Rizzo, Y. Bi, S.D. Dunn, B.H. Shilton, The "second stalk" of *Escherichia coli* ATP synthase: structure of the isolated dimerization domain, Biochemistry 41 (21) (2002) 6875–6884.
[34] S. Wilkens, S.D. Dunn, J. Chandler, F.W. Dahlquist, R.A. Capaldi, Solution structure of the N-terminal domain of the delta subunit of the *E. coli* ATP synthase, Nat. Struct. Biol. 4 (3) (1997) 198–201.
[35] S.D. Dunn, M. Revington, D.J. Cipriano, B.H. Shilton, The *b* subunit of *Escherichia coli* ATP synthase, J. Bioenerg. Biomembranes 32 (4) (2000) 347–355.
[36] A.J.W. Rodgers, S. Wilkens, R. Aggeler, M.B. Morris, S.M. Howitt, R.A. Capaldi, The subunit delta subunit *b* domain of the *Escherichia coli* F(1)F(0)ATPase—the *b* subunits interact with F-1 as a dimer and through the delta subunit, J. Biol. Chem. 272 (49) (1997) 31058–31064.
[37] C. Motz, T. Hornung, M. Kersten, D.T. McLachlin, S.D. Dunn, J.G. Wise, P.D. Vogel, The subunit *b* dimer of the F0F1-ATP synthase interaction with F-1-ATPase as deduced by site-specific spin-labeling, J. Biol. Chem. 279 (47) (2004) 49074–49081.
[38] S. Steigmiller, M. Borsch, P. Graber, M. Huber, Distances between the *b*-subunits in the tether domain of F0F1-ATP synthase from *E. coli*, Biochim. Biophys. Acta Bioenerg. 1708 (2) (2005) 143–153.
[39] M. Revington, D.T. McLachlin, G.S. Shaw, S.D. Dunn, The dimerization domain of the *b* subunit of the *Escherichia coli* F1F0-ATPase, J. Biol. Chem. 274 (43) (1999) 31094–31101.
[40] D.D. Root, V.K. Yadavalli, J.G. Forbes, K. Wangy, Coiled-coil nanomechanics and uncoiling and unfolding of the superhelix and alpha-helices of myosin, Biophys. J. 90 (2006) 2852–2866.
[41] D. Bhatt, S.P. Cole, T.B. Grabar, S.B. Claggett, B.D. Cain, Manipulating the length of the *b* subunit F-1 binding domain in F1F0 ATP synthase from *Escherichia coli*, J. Bioenerg. Biomembranes 37 (2) (2005) 67–74.
[42] P.L. Sorgen, M.R. Bubb, B.D. Cain, Lengthening the second stalk of F1F0 ATP synthase in *Escherichia coli*, J. Biol. Chem. 274 (51) (1999) 36261–36266.
[43] M. Muller, O. Panke, W. Junge, S. Engelbrecht, F-1-ATPase, the C-terminal end of subunit gamma is not required for ATP hydrolysis-driven rotation, J. Biol. Chem. 277 (26) (2002) 23308–23313.
[44] M. Sokolov, L. Lu, W. Tucker, F. Gao, P.A. Gegenheimer, M.L. Richter, The 20 C-terminal amino acid residues of the chloroplast ATP synthase gamma subunit are not essential for activity, J. Biol. Chem. 274 (20) (1999) 13824–13829.
[45] T. Elston, H.Y. Wang, G. Oster, Energy transduction in ATP synthase, Nature 391 (6666) (1998) 510–513.
[46] Z.L. Ni, H. Dong, J.M. Wei, N-terminal deletion of the gamma subunit affects the stabilization and activity of chloroplast ATP synthase, Febs J. 272 (6) (2005) 1379–1385.
[47] H.Y. Wang, G. Oster, Energy transduction in the F-1 motor of ATP synthase, Nature 396 (6708) (1998) 279–282.
[48] G. Oster, H.Y. Wang, ATP synthase: two motors, two fuels, Struct. With Folding Des. 7 (4) (1999) R67–R72.
[49] M.S. Liu, B.D. Todd, R.J. Sadus, Kinetics and chemomechanical properties of the F-1-ATPase molecular motor, J. Chem. Phys. 118 (21) (2003) 9890–9898.
[50] M.S. Liu, B.D. Todd, R.J. Sadus, Dynamic and coordinating domain motions in the active subunits of the F-1-ATPase molecular motor, Biochim. Biophys. Acta Proteins Proteomics 1764 (10) (2006) 1553–1560.
[51] Y. Shirakihara, A.G.W. Leslie, J.P. Abrahams, J.E. Walker, T. Ueda, Y. Sekimoto, M. Kambara, K. Saika, Y. Kagawa, M. Yoshida, The crystal structure of the nucleotide-free alpha 3 beta 3 subcomplex of F-1-ATPase from the thermophilic Bacillus PS3 is a symmetric trimer, Structure 5 (6) (1997) 825–836.
[52] C. Grubmeyer, R.L. Cross, H.S. Penefsky, Mechanism of ATP hydrolysis by beef-heart mitochondrial ATPase. Rate constants for elementary steps in catalysis at a single site, J. Biol. Chem. 257 (20) (1982) 2092–2100.
[53] C. Gibbons, M.G. Montgomery, A.G.W. Leslie, J.E. Walker, The structure of the central stalk in bovine F-1-ATPase at 2.4 Å resolution, Nat. Struct. Biol. 7 (11) (2000) 1055–1061.
[54] V. Kabaleeswaran, N. Puri, J.E. Walker, A.G.W. Leslie, D.M. Mueller, Novel features of the rotary catalytic mechanism revealed in the structure of yeast F-1 ATPase, Embo J. 25 (22) (2006) 5433–5442.
[55] G. Groth, E. Pohl, The structure of the chloroplast F-1-ATPase at 3.2 å resolution, J. Biol. Chem. 276 (2) (2001) 1345–1352.
[56] C. Chen, A.K. Saxena, W.N. Simcoke, D.N. Garboczi, P.L. Pedersen, Y.H. Ko, Mitochondrial ATP synthase—Crystal structure of the catalytic F-1 unit in a vanadate-induced transition-like state and implications for mechanism, J. Biol. Chem. 281 (19) (2006) 13777–13783.
[57] A.V. Syroeshkin, L.E. Bakeeva, D.A. Cherepanov, Contraction transitions of F1-F0 ATPase during catalytic turnover, Biochim. Biophys. Acta 1409 (1998) 59–71.
[58] R.A. Capaldi, B. Schulenberg, The epsilon subunit of bacterial and chloroplast F1F0 ATPases. Structure, arrangement, and role of the epsilon subunit in energy coupling within the complex, Biochim. Biophys. Acta 1458 (2–3) (2000) 263–269.
[59] C.W. Wolgemuth, S.X. Sun, Elasticity of alpha-helical coiled coils, Phys. Rev. Lett. 97 (24) (2006).
[60] T.C. Elston, G. Oster, Protein turbines. 1. The bacterial flagellar motor, Biophys. J. 73 (2) (1997) 703–721.
[61] V.K. Dickson, J.A. Silvester, I.M. Fearnley, A.G.W. Leslie, J.E. Walker, On the structure of the stator of the mitochondrial ATP synthase, Embo J. 25 (12) (2006) 2911–2918.
[62] M.L. Richter, B. Snyder, R.E. Mccarty, G.G. Hammes, Binding stoichiometry and structural mapping of the epsilon-polypeptide of chloroplast coupling factor-1, Biochemistry 24 (21) (1985) 5755–5763.
[63] R.A. Capaldi, R. Aggeler, S. Wilkens, G. Gruber, Structural changes in the gamma and epsilon subunits of the *Escherichia coli* F1F0-type ATPase during energy coupling, J. Bioenerg. Biomembranes 28 (5) (1996) 397–401.
[64] A.J.W. Rodgers, M.C.J. Wilce, Structure of the gamma-epsilon complex of ATP synthase, Nat. Struct. Biol. 7 (11) (2000) 1051–1054.
[65] S.P. Tsunoda, A.J.W. Rodgers, R. Aggeler, M.C.J. Wilce, M. Yoshida, R.A. Capaldi, Large conformational changes of the epsilon subunit in the bacterial F1F0 ATP synthase provide a ratchet action to regulate this rotary motor enzyme, Proc. Natl. Acad. Sci. USA 98 (12) (2001) 6560–6564.
[66] T. Suzuki, T. Murakami, R. Iino, J. Suzuki, S. Ono, Y. Shirakihara, M. Yoshida, F0F1-ATPase/synthase is geared to the synthesis mode by conformational rearrangement of epsilon subunit in response to proton motive force and ADP/ATP balance, J. Biol. Chem. 278 (47) (2003) 46840–46846.
[67] D.J. Cipriano, Y.M. Bi, S.D. Dunn, Genetic fusions of globular proteins to the epsilon subunit of the *Escherichia coli* ATP synthase—implications for in vivo rotational catalysis and epsilon subunit function, J. Biol. Chem. 277 (19) (2002) 16782–16790.
[68] B.A. Feniouk, T. Suzuki, M. Yoshida, The role of subunit epsilon in the catalysis and regulation of F0F1-ATP synthase, Biochim. Biophys. Acta Bioenerg. 1757 (5–6) (2006) 326–338.
[69] M.D. Hossain, S. Furuike, Y. Maki, K. Adachi, M.Y. Ali, M. Huq, H. Itoh, M. Yoshida, K. Kinosita, The rotor tip inside a bearing of a thermophilic F-1-ATPase is dispensable for torque generation, Biophys. J. 90 (11) (2006) 4195–4203.
[70] D. Spetzler, J. York, D. Daniel, R. Fromme, D. Lowry, W.D. Frasch, Microsecond time scale rotation measurements of single F-1-ATPase molecules, Biochemistry 45 (10) (2006) 3117–3124.
[71] K.Y. Hara, H. Noji, D. Bald, R. Yasuda, K. Kinosita, M. Yoshida, The role of the DELSEED motif of the beta subunit in rotation of F-1-ATPase, J. Biol. Chem. 275 (19) (2000) 14260–14623.
[72] G. Gruber, R.A. Capaldi, The trapping of different conformations of the *Escherichia coli* F-1 ATPase by disulfide bond formation—effect of nucleotide binding affinities of the catalytic sites, J. Biol. Chem. 271 (51) (1996) 32623–32628.
[73] R. Aggeler, R.A. Capaldi, Nucleotide-dependent movement of the epsilon subunit between alpha and beta subunits in the *Escherichia coli* F1F0-type ATPase, J. Biol. Chem. 271 (23) (1996) 13888–13891.